Correlation between the transport mechanisms in conductive filaments inside Ta_2O_5-based resistive switching devices and in substoichiometric TaO_x thin films

Carlos M. M. Rosário, Bo Thöner, Alexander Schönhals, Stephan Menzel, Matthias Wuttig, Rainer Waser, Nikolai A. Sobolev, and Dirk J. Wouters

Citation: Appl. Phys. Lett. **112**, 213504 (2018); doi: 10.1063/1.5024504
View online: https://doi.org/10.1063/1.5024504
View Table of Contents: http://aip.scitation.org/toc/apl/112/21
Published by the American Institute of Physics

Correlation between the transport mechanisms in conductive filaments inside Ta_2O_5-based resistive switching devices and in substoichiometric TaO_x thin films

Carlos M. M. Rosário,[1,2,a)] Bo Thöner,[3] Alexander Schönhals,[2] Stephan Menzel,[4] Matthias Wuttig,[3,4] Rainer Waser,[2,4] Nikolai A. Sobolev,[1,5] and Dirk J. Wouters[2]
[1]*Physics Department and I3N, University of Aveiro, Aveiro 3810-193, Portugal*
[2]*Institut für Werkstoffe der Elektrotechnik II, RWTH Aachen University, Aachen 52074, Germany*
[3]*I. Physikalisches Institut IA, RWTH Aachen University, Aachen 52074, Germany*
[4]*Peter Grünberg Institute and JARA-FIT, Forschungszentrum Jülich, Jülich 52428, Germany*
[5]*National University of Science and Technology "MISiS," Moscow 119049, Russia*

(Received 1 February 2018; accepted 3 May 2018; published online 21 May 2018)

Conductive filaments play a key role in redox-based resistive random access memory (ReRAM) devices based on the valence change mechanism, where the change of the resistance is ascribed to the modulation of the oxygen content in a local region of these conductive filaments. However, a deep understanding of the filaments' composition and structure is still a matter of debate. We approached the problem by comparing the electronic transport, at temperatures from 300 K down to 2 K, in the filaments and in TaO_x films exhibiting a substoichiometric oxygen content. The filaments were created in Ta (15 nm)/Ta_2O_5 (5 nm)/Pt crossbar ReRAM structures. In the TaO_x thin films with various oxygen contents, the in-plane transport was studied. There is a close similarity between the electrical properties of the conductive filaments in the ReRAM devices and of the TaO_x films with $x \sim 1$, evidencing also no dimensionality difference for the electrical transport. More specifically, for both systems there are two different conduction processes: one in the higher temperature range (from 50 K up to ~300 K), where the conductivity follows a $\sqrt{T}$ dependence, and one at lower temperatures (<50 K), where the conductivity follows the $\exp(-1/\sqrt{T})$ dependence. This suggests a strong similarity between the material composition and structure of the filaments and those of the substoichiometric TaO_x films. We also discuss the temperature dependence of the conductivity in the framework of possible transport mechanisms, mainly of those normally observed for granular metals. *Published by AIP Publishing.* https://doi.org/10.1063/1.5024504

The resistive switching (RS) phenomenon paves the way for a new generation of nonvolatile memories, known as redox-based resistive random access memories (ReRAMs).[1] This technology is among the strongest candidates for application as storage-class memory, whose purpose is to bridge the gap between the fast, volatile DRAM, used for memory and computations, and the slower, non-volatile NAND-Flash, used for storage.[2] ReRAMs also appear in the front-line for application in neuromorphic devices that enable new paradigms of computing[3] and, more generally, as memristive systems, considered a capable building block for future electronics.[4] The valence-change mechanism (VCM) is one of the main models to explain the RS in metal-insulator-metal structures with transition metal oxides.[1] This mechanism is based on redox reactions that modulate the oxygen content in a local region of an oxygen-deficient conductive filament. The filament's conductivity is dependent on its oxygen content. Although research on VCM systems has led to a better understanding of the switching mechanism,[1,5] the switching kinetics,[5,6] and the materials to choose from,[7] there are still open questions that hinder the development of better design rules for device fabrication. Among these, the composition and structure of the conductive filaments and their impact on the transport in the devices in the different resistive states are still a matter of debate. Due to the nanoscale dimensions of the filaments, it proves very challenging to study these objects using conventional methods for composition and structure determination. For that reason, we focus on the electronic transport properties as a tool to gain information on the filaments. Accordingly, we measured the electrical transport from 300 K down to 2 K for different low-resistance states (LRS) of Ta (15 nm)/Ta_2O_5 (5 nm)/Pt crossbar ReRAM devices and compared the results to the ones from similar measurements performed on thin films of TaO_x with different substoichiometric compositions. In this letter we show, over the whole temperature range, a clear correlation between the conduction in the filaments and in the TaO_x films with $x \sim 1$.

The RS proceeds typically between two different resistance states: a low-resistance state (LRS) or "ON" state and a high-resistance state (HRS) or "OFF" state. This work deals with the conduction in the LRS, where, according to most of the existing device models, there is a conductive filament connecting the electrodes. In general, the conduction in microstructured devices can be limited by interfacial or bulk conduction processes. To describe the HRS, the proposed models are based on the narrowing of the filament (bulk-limited), such as the quantum point contact model,[8] or on the existence of an interfacial barrier (interface-limited).[5,9]

a)Author to whom correspondence should be addressed: cmiguelrosario@ua.pt

However, the conduction in the filament is thought to be the dominant conduction process in the LRS.[5] This is corroborated by the common use of bulk conduction mechanisms to fit the conduction in the LRS.[10–14]

Tantalum oxide (Ta_2O_5 or more generally TaO_x) is one of the most popular transition metal oxides used as an insulator in metal-insulator-metal structures for ReRAM devices, showing high endurance[15] and high switching speed.[16] The conduction in the LRS of Ta_2O_5-based ReRAM devices has been ascribed to metallic conduction or to hopping processes, below room temperature.[10,12,14] However, these hopping mechanisms lead to unrealistic parameters. More specifically, they assume hopping distances such as 0.16 nm (Ref. 12) that are smaller than the reported minimum interatomic distance of 0.19 nm in amorphous Ta_2O_5.[17] A distance of 0.3 nm between oxygen vacancies (hopping sites)[14] contradicts the hopping mechanisms involving localized energy levels. Therefore, different mechanisms for the transport in conductive filaments should be considered. The connection between the conduction in Ta_2O_5 ReRAM devices and in substoichiometric TaO_x films was previously reported. Miao *et al.*[18] compared both cases based on the temperature coefficient of resistance (TCR) in a limited temperature range from 250 K to 300 K. Graves *et al.*[14] refer to their previous study on the conduction in TaO_x films[19] when justifying the choice of the conduction mechanism down to 100 K. However, a comparison of the transport properties of Ta_2O_5 ReRAM devices and of substoichiometric TaO_x thin films for temperatures down to 2 K has never been reported. The low temperatures could enable the observation of quantum interference effects such as weak localization or electron-electron interactions, normally not observable at higher temperature due to dominant phonon scattering. The occurrence or absence of these effects can lead to important information, similarly to what has been reported for phase-change materials.[20] We did not explore temperatures above room temperature in order to avoid conduction through the insulating Ta_2O_5 layer in parallel to the conductive filament, which could hinder the study of the filament.[14]

The $Ta/Ta_2O_5/Pt$ ReRAM devices used in this work were fabricated by radiofrequency (RF) magnetron sputtering of all layers in an inert Ar atmosphere for the metal layers or in a reactive Ar and O_2 mixture for the oxide layers. A second Pt layer is used to cap the Ta top electrode to avoid oxidation. Both Pt layers are 20 nm thick, while the Ta layer is 15 nm and the Ta_2O_5 layer is 5 nm thick. The samples were patterned into crossbar devices with lateral sizes of 5, 10, and 25 μm, as schematically depicted in Fig. 1(a). The substoichiometric TaO_x thin films were sputtered from a Ta target in an atmosphere of Ar and O_2. The oxygen content was tuned by modifying the O_2-to-Ar ratio, the chamber pressure, and the RF power. The TaO_x layers have a thickness of 20 nm and were patterned in a van der Pauw structure with Pt electrodes. To avoid oxidation when exposed to air, the TaO_x films were capped *in situ* with a 20 nm Al_2O_3 layer. The composition of the layers was determined through Rutherford backscattering spectrometry. A complete description of the sample preparation and methods used is given in the supplementary material.

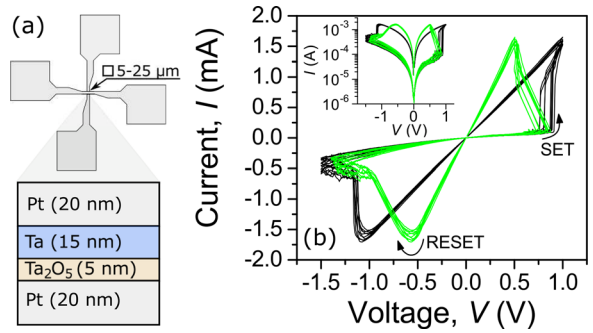

FIG. 1. (a) Schematic depiction of the crossbar $Ta/Ta_2O_5/Pt$ ReRAM devices used in this work. (b) Typical quasi-static current-voltage (*I-V*) characteristics measured at room temperature for the devices (10 cycles). The black lines show the measured *I-V* characteristics, while the green lines show the *I-V* characteristics with the voltage drop at the series resistance subtracted. The inset shows the data plotted on a logarithmic scale for the current.

The Ta_2O_5 ReRAM devices show the typical bipolar RS of VCM systems, as can be seen in the quasi-static current-voltage (*I-V*) characteristics measured at room temperature [Fig. 1(b)]. During the *I-V* measurements, the voltage was applied to the Ta top electrode, while the Pt bottom electrode was grounded. The devices were self-complied by the series resistance of the crossbar metal lines, and no current compliance was used during the switching. The series resistance is around 500 Ω for the 5×5 μm^2 devices. The devices are initialized with an electroforming step accomplished at +2 V, after which the devices switch between the LRS and the HRS. The LRS ranged from 250 Ω to 3 kΩ, while the HRS ranged from 5 kΩ to 40 kΩ. Nevertheless, the resistance ratio, defined as R_{HRS}/R_{LRS}, was always larger than 10. To obtain an estimate of the real ("intrinsic") switching voltage, the voltage drop over the series resistance was subtracted,[21] yielding the switching curves shown in green in Fig. 1(b). The *I-V* characteristics are typically linear in the LRS and nonlinear in the HRS. The linearity of the LRS (also observed at 2 K, see supplementary material) precludes a strong (presumed) nonlinear effect of contact resistances at the electrodes and shows that there is no significant effect of the electric field on the conduction mechanism for this state up to the switching voltage.

After at least 10 switching cycles, the devices were set to the LRS, and their resistance was measured as a function of temperature from 300 K down to 2 K in a cryostat. The resistance was measured at a fixed current value in a 4-wire configuration to exclude the series resistance and only probe the Ta/Ta_2O_5 stack. For more detailed information on the measurement method and parasitic effect investigation, see supplementary material. The temperature dependent resistance curves typically observed are shown for two different devices in Fig. 2. The resistance decreases with increasing temperature, exhibiting a negative temperature coefficient of resistance (TCR). The temperature dependence is very weak, with the resistance changing by less than 10% from 300 K to 2 K. Also, the resistance is clearly not diverging strongly at low temperatures, evidencing metal-like behavior. However, this behavior is not the one observed in ordinary metals with a positive TCR. This fact is more clearly observed in the reduced activation energy plots[22] shown in Fig. S5(a) of the supplementary material.

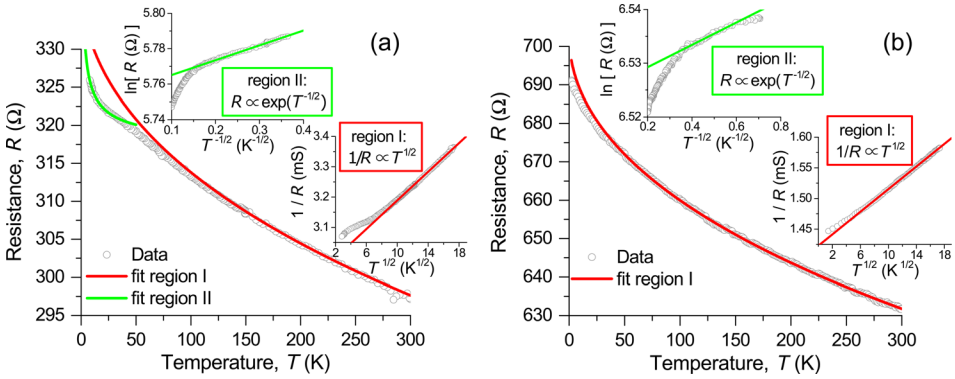

FIG. 2. [(a), (b)] Resistance as a function of the temperature for two different Ta/Ta_2O_5/Pt devices in the low resistance state. The colored curves are results of the least squares fitting in two different temperature ranges. The insets show the data in the linearized plots for the high- and low-temperature regimes mentioned in the text.

For some of the devices, a distinctive change in the behavior of the R vs. T curve is observed below 50 K, visible in Fig. 2(a). This divides the R vs. T curve into two regions. Fitting possible conduction mechanisms to the data clearly reveals the existence of two different regimes. In the high-temperature regime, for $50\,\mathrm{K} < T < 300\,\mathrm{K}$, the best fit to the data is obtained with a $\sqrt{T}$ dependence of the conductance. In the low-temperature regime, at $T < 50\,\mathrm{K}$, an exp $(1/\sqrt{T})$ dependence gives a good fit for the resistance [see the insets of Fig. 2(a)]. For other devices, as exemplified by the curve in Fig. 2(b), the same low temperature regime is less clearly observed. However, the high-temperature regime is maintained until lower temperatures (below 50 K), indicating that, if existent, the transition between the two regions is shifted down on the temperature scale.

The substoichiometric TaO_x thin films show an increase in the (room temperature) resistivity with the increasing oxygen content. The inset of Fig. 3(a) displays the data for TaO_x films with x ranging from 1 to 1.5. This is the range of compositions where the resistivity is expected to start changing more drastically.[23] At higher oxygen contents, the resistivity ran out of the measurement range of the van der Pauw setup. Figure 3(a) shows the resistivity as a function of temperature for three different compositions in the mentioned interval. The temperature dependence of the resistivity is qualitatively similar for all compositions shown, being rather weak for most of the temperature range from 300 K down to approximately 50 K and getting stronger at lower temperatures, especially with increasing x.

A comparison between the curves in Fig. 3(a) and the one in Fig. 2(a) shows a striking similarity in the temperature dependence of the resistivity for $x \sim 1$ in the temperature range from 10 K to 300 K. To elucidate this correspondence, we chose the TaO_x film with $x \sim 1$, displayed in the graph of Fig. 3(b). This film shows a rather low resistivity of $2 \times 10^{-5}\,\Omega\,\mathrm{m}$ at room temperature. This value is an order of magnitude higher than that of a sputtered Ta film with $10^{-6}\,\Omega\,\mathrm{m}$, but several orders of magnitude lower than in amorphous Ta_2O_5 that can reach 10^5 to $10^7\,\Omega\,\mathrm{m}$.[24] Once more, we observe the same distinctive behavior measured for the devices, separating two temperature regions, where the conductivity follows the $\sqrt{T}$ and $\exp(-1/\sqrt{T})$ dependences [see the insets of Fig. 3(b)]. It can be observed, however, that in the very low temperature range, below 10 K, a deviation from the $\exp(-1/\sqrt{T})$ behavior occurs, which is not observed for the devices. We believe that this deviation can be ascribed to weak antilocalization. The same two regimes can be fitted to the resistivity of the film with $x \sim 1.5$ (see Fig. S7 in the supplementary material). However, the temperature range where the $\exp(-1/\sqrt{T})$ behavior is observed is wider compared to the film with $x \sim 1$, now reaching up to almost 100 K. This is an indication that the composition plays a role in determining the temperature at which the transition between the two regimes takes place.

The observed correlation between the transport in conductive filaments in Ta_2O_5 devices and TaO_x thin films can seem rather strange at first sight, as the dimensionality for transport could be different. However, first, the relatively high current measured in the devices indicates a rather thick filament, possibly enabling 3D "bulk" transport. Second, if we consider the case of a conductive filament of a

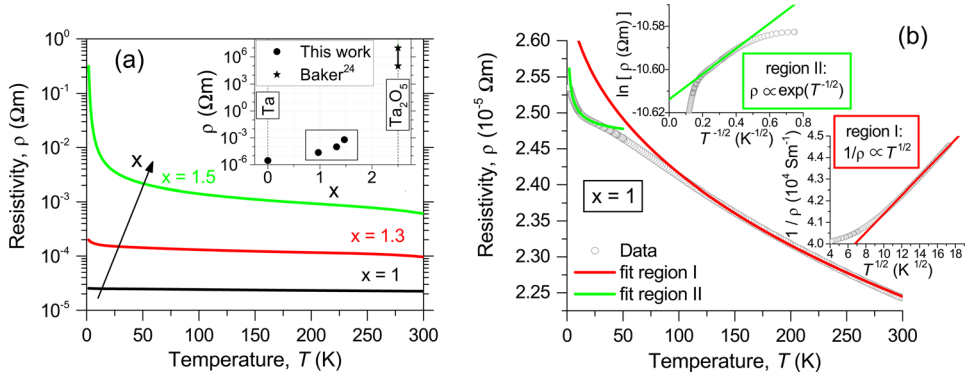

FIG. 3. (a) Resistivity as a function of temperature for TaO_x films with x = 1–1.5. The inset shows the room temperature resistivity as a function of x for the TaO_x films with x = 1–1.5, a sputtered Ta film and literature values for Ta_2O_5 from Ref. 24. (b) Temperature dependence of the resistivity for the TaO_x film with x = 1 with the results of the least squares fits to the data, evidencing two temperature ranges with different temperature dependences of the resistivity. The insets show the data in the linearized plots.

homogeneous material with the nanometric dimensions usually considered, we could have 1D transport, as it is sometimes discussed.[25] This could indeed cause problems in the comparison with the possible 2D transport in the case of homogeneous TaO_x films. However, the TaO_x system is reported to have only two stable solid phases: Ta(O) solid solution and Ta_2O_5.[26] This would then mean that the TaO_x films are a mixture of metallic Ta(O) and insulating Ta_2O_5. This is similar to the case of granular metals, where the dimensionality is given by the spatial distribution of the metallic grains.[27,28] As we did not intentionally induce a lower dimensionality of the distribution of the Ta grains during the sputtering of the TaO_x thin films and the electroforming of the devices, we could have a 3D array of small metallic particles. X-ray diffraction measurements on the TaO_x films (see supplementary material) show evidence of the existence of Ta in the disordered β-Ta phase,[29] and the broadening of the reflection peaks compared to a Ta film could indicate smaller crystallites in the TaO_x films. 100 nm thick TaO_x films with $x = 1$ exhibit the same behavior displayed in Fig. 3(b) for 20 nm films, thus excluding both a dimensionality difference between both films and a relevant contribution from surface effects.

The temperature dependence of the LRS in Ta_2O_5-based ReRAM devices was previously ascribed to nearest-neighbor hopping at higher temperatures (100–300 K)[10,12,14] and variable-range hopping at lower temperatures (down to 5 K).[10,12] However, these mechanisms are not suitable to explain the behavior in the whole temperature range from 2 K to 300 K (see supplementary material), and the respective fittings yield physically unreasonable parameters.

The $\sqrt{T}$ dependence of the conductivity that we fitted in the temperature range from 50 K to 300 K is commonly observed for the conduction in disordered metals, also known as dirty metals.[30,31] This stems from a quantum correction to the conductivity given by the Boltzmann transport equation due to electron-electron interference, the so-called Al'tshuler-Aronov effect.[32] This correction is given by[31]

$$\Delta\sigma = A_{e-e}\sqrt{T}, \tag{1}$$

where A_{e-e} is a factor dependent on the electron diffusion and on the strength of the screening between electrons. Such a behavior is also observed when there is a percolation path between granules of disordered metals.[27] However, the observed $\sqrt{T}$ dependence could also arise from a different transport mechanism. Huth *et al.*[33] report a similar power law dependence of the conductivity for the case of W-based granular metals in the metallic regime. These authors mention the possibility of having a coherent tunneling percolation path, based on the theory by Beloborodov *et al.*[34] This mechanism can be, above a certain critical temperature, independent of the dimensionality of the granular metal.

The resistivity dependence of the form $\exp(1/\sqrt{T})$, which we fitted for temperatures below 50 K, is characteristic of Efros-Shklovskii variable range hopping, where a strong Coulomb interaction between the charge carriers leads to a resistivity of the form[35]

$$\rho = \rho_0 \exp\left(\sqrt{T_0/T}\right), \tag{2}$$

with ρ_0 and T_0 being constants. The same temperature dependence is also observed for granular metals in the insulating regime, i.e., below the percolation threshold.[27]

Finally, if we take the resistivity measured in the TaO_x films with $x \sim 1$ and calculate the resistance for a cylindrical filament with a typical diameter of 10 nm (Ref. 5) and a length of 5 nm, we obtain a resistance of 1.5 kΩ. This resistance fits in the measured resistance interval for the LRS, which further corroborates the assumption that the current in the LRS is controlled by the bulk conduction in the filament.

In summary, we have presented clear correlations between the electrical transport in conductive filaments in Ta_2O_5-based ReRAM devices in the low-resistance state and the in-plane transport in substoichiometric TaO_x thin films with $x \sim 1$ in the temperature range spanning from 2 K to 300 K. The temperature dependence of the conductivity can be divided into two regimes fitted by two different functions: at $T \gtrsim 50$ K, the conductivity follows a $\sqrt{T}$ dependence, while at $T \lesssim 50$ K, it obeys an $\exp(-1/\sqrt{T})$ law. This also indicates that the dimensionality of conduction is similar in both systems. This could originate from the relatively thick conductive filaments associated with the operation of the ReRAM devices at currents up to 2 mA, possibly enabling 3D-like transport. Another reason could be the discussed similarity with the transport mechanisms observed in granular metals, where the dimensionality is determined by the spatial distribution of the metallic granules. The correlations obtained for both regimes provide strong evidence that the physical mechanisms responsible for the conduction in both cases are the same. This suggests a close similarity between the material properties of the conductive filaments in the devices and of the substoichiometric TaO_x films. This finding motivates further detailed analytical studies on substoichiometric TaO_x films, as they may provide a much needed insight into the composition and structure of the conductive filaments in the Ta_2O_5 ReRAM devices.

See supplementary material for more details on sample fabrication, measurement procedures, and additional supporting data.

C.M.M.R. thanks the FCT of Portugal and the DAEPHYS for the studentship PD/BD/105917/2014. C.M.M.R. and N.A.S. acknowledge financial support of the FCT through the Project No. I3N/FSCOSD (Ref. FCT UID/CTM/50025/2013). We thank the DFG for financial support through the Collaborative Research Centre SFB 917 "Nanoswitches." We also thank the CRUP and the DAAD for the Portuguese-German Integrated Action A-14/17. We would like to thank Nuno Barradas and Eduardo Alves from C^2TN, IST-University of Lisbon for RBS measurements and Johannes Reindl from I. Physikalisches Institut IA, RWTH for assistance in the electrical transport measurements.

[1]R. Waser, R. Dittmann, G. Staikov, and K. Szot, Adv. Mater. **21**, 2632 (2009).
[2]G. W. Burr, B. N. Kurdi, J. C. Scott, C. H. Lam, K. Gopalakrishnan, and R. S. Shenoy, IBM J. Res. Dev. **52**, 449 (2008).
[3]D. S. Jeong, K. M. Kim, S. Kim, B. J. Choi, and C. S. Hwang, Adv. Electron. Mater. **2**, 1600090 (2016).
[4]M. A. Zidan, J. P. Strachan, and W. D. Lu, Nat. Electron. **1**, 22 (2018).

[5]A. Marchewka, B. Roesgen, K. Skaja, H. Du, C. L. Jia, J. Mayer, V. Rana, R. Waser, and S. Menzel, Adv. Electron. Mater. **2**, 1500233 (2016).
[6]S. Menzel, M. Waters, A. Marchewka, U. Böttger, R. Dittmann, and R. Waser, Adv. Funct. Mater. **21**, 4487 (2011).
[7]H. S. P. Wong, H. Y. Lee, S. Yu, Y. S. Chen, Y. Wu, P. S. Chen, B. Lee, F. T. Chen, and M. J. Tsai, Proc. IEEE **100**, 1951 (2012).
[8]R. Degraeve, A. Fantini, N. Raghavan, L. Goux, S. Clima, Y. Y. Chen, A. Belmonte, S. Coseman, B. Govoreanu, D. J. Wouters, P. Roussel, G. S. Kar, G. Greseneken, and M. Jurczak, in *Proceedings of the 21th International Symposium on the Physical and Failure Analysis of Integrated Circuits (IPFA) (IPFA)*, Marina Bay Sands, Singapore, 30 June–4 July 2014 (IEEE, 2014), pp. 245–249.
[9]A. Marchewka, R. Waser, and S. Menzel, in *2015 International Conference on Simulation of Semiconductor Processes and Devices (SISPAD)*, Washington, DC, USA, 9–11 September 2015 (IEEE, 2015), pp. 297–300.
[10]Z. Wei, T. Takagi, Y. Kanzawa, Y. Katoh, T. Ninomiya, K. Kawai, S. Muraoka, S. Mitani, K. Katayama, S. Fujii, R. Miyanaga, Y. Kawashima, T. Mikawa, K. Shimakawa, and K. Aono, in *2011 IEEE International Electron Devices Meeting*, Washington, DC, USA, 5–7 December 2011 (IEEE, 2011), pp. 721–724.
[11]F. De Stefano, M. Houssa, V. V. Afanas'ev, J. A. Kittl, M. Jurczak, and A. Stesmans, Thin Solid Films **533**, 15 (2013).
[12]Y. Zhang, N. Deng, H. Wu, Z. Yu, J. Zhang, and H. Qian, Appl. Phys. Lett. **105**, 063508 (2014).
[13]R. Fang, W. Chen, L. Gao, W. Yu, and S. Yu, IEEE Electron Device Lett. **36**, 567 (2015).
[14]C. E. Graves, N. Dávila, E. J. Merced-Grafals, S. Lam, J. P. Strachan, and R. S. Williams, Appl. Phys. Lett. **110**, 123501 (2017).
[15]M. J. Lee, C. B. Lee, D. Lee, S. R. Lee, M. Chang, J. H. Hur, Y. B. Kim, C. J. Kim, D. H. Seo, S. Seo, U. I. Chung, I. K. Yoo, and K. Kim, Nat. Mater. **10**, 625 (2011).
[16]A. C. Torrezan, J. P. Strachan, G. Medeiros-Ribeiro, and R. S. Williams, Nanotechnology **22**, 485203 (2011).
[17]R. Bassiri, F. Liou, M. R. Abernathy, A. C. Lin, N. Kim, A. Mehta, B. Shyam, R. L. Byer, E. K. Gustafson, M. Hart, I. MacLaren, I. W. Martin, R. K. Route, S. Rowan, J. F. Stebbins, and M. M. Fejer, APL Mater. **3**, 036103 (2015).
[18]F. Miao, W. Yi, I. Goldfarb, J. J. Yang, M. Zhang, M. D. Pickett, J. P. Strachan, G. Medeiros-Ribeiro, and R. S. Williams, ACS Nano **6**, 2312 (2012).
[19]I. Goldfarb, F. Miao, J. J. Yang, W. Yi, J. P. Strachan, M.-X. Zhang, M. D. Pickett, G. Medeiros-Ribeiro, and R. S. Williams, Appl. Phys. A **107**, 1 (2012).
[20]N. P. Breznay, H. Volker, A. Palevski, R. Mazzarello, A. Kapitulnik, and M. Wuttig, Phys. Rev. B **86**, 205302 (2012).
[21]A. Fantini, D. J. Wouters, R. Degraeve, L. Goux, L. Pantisano, G. Kar, Y.-Y. Chen, B. Govoreanu, J. A. Kittl, L. Altimime, and M. Jurczak, in *2012 IEEE International Memory Workshop*, Milan, Italy, 20–23 May 2012 (IEEE, 2012), pp. 1–4.
[22]A. G. Zabrodskii and K. N. Zinov'eva, Sov. Phys. JETP **59**, 425 (1984), available at http://www.jetp.ac.ru/cgi-bin/e/index/e/59/2/p425?a=list.
[23]Z. Wei, Y. Kanzawa, K. Arita, Y. Katoh, K. Kawai, S. Muraoka, S. Mitani, S. Fujii, K. Katayama, M. Iijima, T. Mikawa, T. Ninomiya, R. Miyanaga, Y. Kawashima, K. Tsuji, A. Himeno, T. Okada, R. Azuma, K. Shimakawa, H. Sugaya, T. Takagi, R. Yasuhara, K. Horiba, H. Kumigashira, and M. Oshima, in *2008 IEEE International Electron Devices Meeting*, San Francisco, CA, USA, 15–17 December 2008 (IEEE, 2008), pp. 293–296.
[24]P. Baker, Thin Solid Films **14**, 3 (1972).
[25]D. Ielmini, Semicond. Sci. Technol. **31**, 063002 (2016).
[26]S. P. Garg, N. Krishnamurthy, A. Awasthi, and M. Venkatraman, J. Phase Equilib. **17**, 63 (1996).
[27]I. S. Beloborodov, A. V. Lopatin, V. M. Vinokur, and K. B. Efetov, Rev. Mod. Phys **79**, 469 (2007).
[28]Y. Wang, C. Duan, L. Peng, and J. Liao, Sci. Rep. **4**, 7565 (2014).
[29]W. D. Westwood and N. Waterhouse, J. Appl. Phys. **42**, 2946 (1971).
[30]M. A. Howson and D. Greig, Phys. Rev. B **30**, 4805 (1984).
[31]P. A. Lee and T. V. Ramakrishnan, Rev. Mod. Phys. **57**, 287 (1985).
[32]B. L. Altshuler and A. G. Aronov, Solid State Commun. **30**, 115 (1979).
[33]M. Huth, D. Klingenberger, C. Grimm, F. Porrati, and R. Sachser, New J. Phys. **11**, 033032 (2009).
[34]I. S. Beloborodov, K. B. Efetov, A. V. Lopatin, and V. M. Vinokur, Phys. Rev. Lett. **91**, 246801 (2003).
[35]V. F. Gantmakher, *Electrons and Disorder in Solids* (Oxford University Press, New York, 2005).